International Journal of Engineering Inventions
e-ISSN: 2278-7461, p-ISSN: 2319-6491
Volume 13, Issue 12 [December. 2024] PP: 22-36

Performance evaluation analysis and structure optimization of dissolvable metal plug slip for shale oil and gas development

Zhen Chen[1,2,3,*], Chaocheng Wei[1], Xiaoyang Ying[1], Qingjie Ran[1],Shuang Jing[1], Zhiqiang Huang[1], Nan Luan[4]

[1]*College of Mechanical and Electrical Engineering, Southwest Petroleum University, Chengdu 610500, China.*

[2]*Sichuan Key Laboratory of Shale Gas Evaluation and Exploitation, Chengdu 610500, China .*

[3]*Oil and gas equipment technology Sharing and Service Platform of Sichuan Province, Chengdu, Sichuan, 610500, P.R. China .*

[4]*Baker Hughes(Malaysia) 25th floor, Menara Tan & Tan 207, Jalan Tun Razak 50400 Kuala Lumpur, Malaysia.*

Abstract:*In the process of volume fracturing of tight oil and gas horizontal wells, the dissovlable metal plug(DMP) has become a key tool for plugging under pressure due to its advantages of rapid solubility, full-bore production and simple construction technology. Slips are the core components to achieve interstage anchoring, and their anchoring quality can determine the success or failure of horizontal fracturing operations. However, the failure of plug setting occurs frequently due to structural fracture and uneven anchoring force of slips during volume fracturing. Therefore, in this paper, finite element analysis and structural optimization research are carried out for the anchoring performance of DMP slips. slip anchoring performance evaluation system was established with the strength criterion, the maximum contact pressure criterion and the contact uniformity criterion as the evaluation indicators.Using finite element simulation technology, the mechanical properties of slips during the anchoring process were studied, and the anchoring performance was evaluated and analyzed.The results show that under the action of 9t setting force, the maximum stress of the slip nail is 1930MPa, and the maximum stress of the slip block is 832MPa, the force is more uniform, and the anchoring performance is better.Based on this, the optimal design of the slip crest angle and tooth inclination angle of the slip block was carried out. After optimization, the single slip can be safely anchored under the action of the standard 1.5t setting force, and the contact pressure distribution is relatively uniform, which meets the anchoring requirements. The safety and anchoring performance of the dissovlable plug structure are improved, and the theoretical basis for the improved design of the dissovlable plug slip structure is provided.*

Key Words: *Staged volume fracturing in horizontal wells; Dissovlable metal plug; Slips; Simulation analysis; Structural optimization*

Date of Submission: 28-11-2024 Date of acceptance: 07-12-2024

---

1. Introduction

With the massive consumption of oil and gas resources, there is an urgent need to increase the exploration and development of oil and gas resources and improve oil and gas production. However, conventional oil and gas resources can no longer meet the demand, and unconventional resources represented by shale gas and tight oil and gas are gradually becoming the mainstay of oil and gas production. Due to the poor physical condition of unconventional reservoir and heterogeneity of formation cracks, it is difficult to explore resources by conventional hydraulic fracturing method[1]. Staged volume fracturing technology is a key technology for efficient development in tight oil and gas reservoirs, whose dissolvable metal plug(DMP) has rapidly become popular in volume fracturing operations because of its fast dissolvability, full-throughput production, and simple construction process, leading the revolutionary progress of horizontal well segmentation and multi-cluster fracturing technology. However, in the volumetric fracturing segmentation transformation operation, the DMP is subjected to shock and vibration, and the anchoring between the casing and the casing may loosen, resulting in increased downward movement of the DMP or even slippage and leakage of the seal, and the casing may also break teeth under large loads leading to anchoring failure,The rupture of slip and casing is shown in Figure

*Corresponding author; Professor， email:971857707@qq.com

1. Therefore, in this paper, the anchoring performance analysis is carried out for the DMP mount shackle structure, and the finite element simulation study of the anchoring performance of the DMP mount shackle is carried out.

Fig. 1. Rupture of slip and casing.

For the seating performance of downhole seal tool slip during operation, the main research methods are indoor tests, finite element analysis studies, and theoretical studies. In terms of theory, Xin Sun et al. obtained the calculation formula of contact force between slip and casing by mechanical analysis, established the finite element model of slip system consisting of slip and casing, and derived the depth of slip bit into casing and the interaction law of slip and casing[2]. Yihua Dou et al. used the thick-wall theory to derive the maximum hoop stress in the inner wall of the casing, and the strength theory to find the ultimate seating force of the casing[3]. In terms of experimental research, Bin Liu used indoor tests to obtain the range of anchoring loads for a certain type of packer shackle[4]. Chao Zheng et al. explored the process of slip formation. The effects of key structural parameters such as top angle, inclination angle and wedge angle on slip contact characteristics were systematically investigated[5]. Zhu Xiaohua et al. conducted seating and sealing tests for the Y440 type packer and found that the tool had a downward movement during the sealing process. They then established a finite element model based on the nonlinear explicit dynamic analysis method to analyze the effect of different slip tooth parameters on the anchoring effect [6].In finite element research, Jia-Yuan Chen et al. used finite element software to analyze the stress distribution in the slip and found that the middle part of the slip structure is the main part that bites into the casing[7]. Yang Tang established a finite element model for the damage of casing pressure on the slip after making wind, and optimized the shackle parameters[8]. Qu established a finite element model of the double rubber cartridge and studied the effect of the friction factor of the sealing element on the sealing system performance using the orthogonal test method; it was found that reducing the friction factor between the casing and the rubber cartridge can effectively avoid the damage of the rubber cartridge [9]. LI et al. designed Y422 recoverable bridge plugs for the development of poor and thin oil reservoirs in the Daqing oilfield and carried out finite element analysis of the structural work of the slip to obtain the stress distribution law [10]. ZHANG et al. designed a hydraulic pumping degradable bridge plug structure and analyzed its sealing performance, anchorage performance, and fluid erosion characteristics using numerical simulation [11]. Wang et al. proposed a structural optimization method that organically combines the finite element method, orthogonal experimental method, BP network, and improved genetic algorithm for slip parameters, which has some engineering guidance for the optimization of slip structural parameters [12]. Yuan Wang analyzed the contact pressure between the slip and casing by finite element software and obtained stress-displacement striation diagrams, which provided guidance for shackle optimization design[13].

In this paper, a mechanical model analysis is established for the DMP cavity structure, and a finite element simulation study of anchoring performance is carried out. The influence of tooth top angle and tooth inclination angle on the anchoring performance of the shackle is discussed, the structure of the soluble ball mount shackle is improved, the metal anchoring performance of the soluble ball mount is improved, and the improved soluble ball mount anchoring performance can meet the requirements of horizontal well fracturing operations.

2. Mechanisms of action and force analysis of dissolvable plug slip

2.1 Analysis of the working process of DMP slip

The dissolvable plug slip is shown in Figure 2, and the multi-flap tile is evenly distributed along the circumference. The slip base is set with a hard slip block with a hoop ring on the outside for stable movement and an inner tapered surface in contact with the sliding body. The tailstock has guide slots to limit the movement of the shackle in the radial direction. When the DMP is seated, the sliding body and the tail seat are subjected to relative motion by the seating force of the seating tool. The inner side of the cavity is squeezed by the sliding body and moves radially to make contact with the casing, and the hard cavity block bites into the wall of the casing to realize the anchoring of the DMP. Sliding body movement to a certain distance when the sliding body is on the horse tooth buckle and tailstock is on the horse tooth buckle with the lock can dissolve the DMP to complete the seat seal.

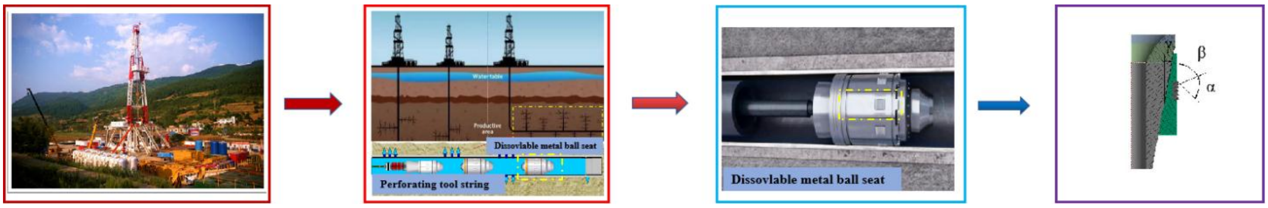

Fig. 2. Tight oil and gas volumetric fracturing process and soluble ball holder tool.

2.2 Analysis of the force on the DMP mount slip

The slip plays an anchoring role during the seating and fracturing of the DMP, fixing the DMP to the casing, preventing the DMP from moving axially along the casing, and ensuring the seal of the DMP. In the process of DMP work, the slip break or cause serious damage to the casing wall, which may cause safety accidents and pose a serious threat to the safe production of oil and gas. Therefore, it is necessary to analyze and study the force on the DMP mount slips. The DMP slip has multiple flaps. Now, we consider a flap chuck and perform a force analysis on it, the structure and force of the chuck are shown in Figure 3.

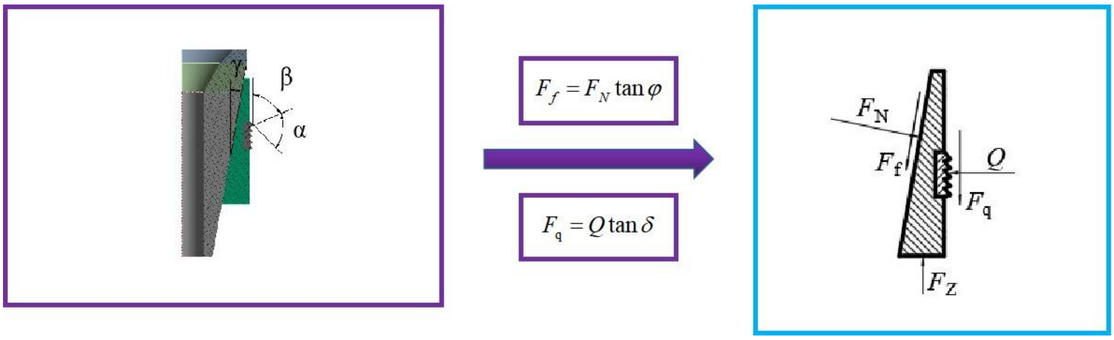

Fig. 3. Single-flap slip structure and force situation.

When the DMP is seated, the slip is subjected to the pressure of the casing wall, the positive pressure given by the sliding body, the frictional force between the sliding body and the tail seat, and the seating force given by the tail seat to the single cavity. From the principle of statics, it is known that the force on the slip should satisfy the following equation:

$$Q = F_N \cos\gamma - F_f \sin\gamma \tag{1}$$

$$F_z - F_q = F_N \sin\gamma + F_f \cos\gamma \tag{2}$$

$$F_f = F_N \tan\varphi \tag{3}$$

Among others，

$$F_Z = W_z / n \tag{4}$$

$$F_q = Q\tan\delta \tag{5}$$

Where: Q — Radial load on the interaction between the single-flap slip and the inner wall of the casing, N.

F_N — Positive pressure of the sliding body on the single-flap slip, N.

F_f —Friction between the sliding body and the single-flap slip, N.

F_z — Sealing force on single valve slip, N.

F_q — Friction between single-flap slip and casing, N.

W_Z — DMP seating load, N.

γ — Tilt angle of contact surface between the slip and sliding body, °

φ — Friction angle between slip and sliding body, °.

n — Number of slip pieces.

From equation (1), equation (2), equation (3), equation (4), and equation (5), we have:

$$Q = \frac{W_Z / n - Q\tan\delta}{\tan(\gamma + \varphi)} \tag{6}$$

where, δ — The friction angle between the cavity and the casing wall, °.

The formula (6) is transformed to obtain:

$$Q = \frac{W_Z}{n\left(\tan(\gamma + \varphi) + \tan\delta\right)} \tag{7}$$

contact pressure between the slip teeth and the casing wall when they are occluded:

$$\sigma = \frac{Q}{A} \tag{8}$$

where， σ — contact pressure between the slip teeth and the inner wall of the casing, N/mm2.

A — Contact area between the slip teeth and the inner wall of the casing, mm2.

From the structure of the slip shown in Figure 2, it can be seen that the contact area between the slip and the inner wall of the casing is:

$$A = ma\frac{\theta \pi D_t}{360}\left(\frac{1}{\tan\beta} + \tan\left(\alpha + \beta - \frac{\pi}{2}\right)\right) \tag{9}$$

where， m — Number of single flap slip teeth.

a — slip teeth bite into the casing.

θ — Single-flap slip with rounded corners.

D_t — Casing inner wall diameter.

α —slip tooth top corner.

β — slip tooth inclination.

From equation (8) and equation (9), we can get:

$$\sigma = \frac{360W_Z}{n(\tan(\gamma + \varphi) \bullet ma\theta \pi D_t)\left(\frac{1}{\tan\beta} + \tan\left(\alpha + \beta - \frac{\pi}{2}\right)\right)} \tag{10}$$

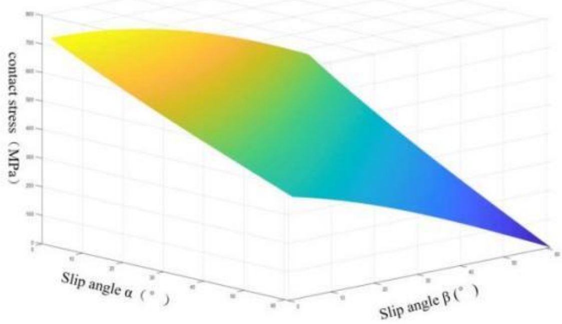

Fig. 4. Three-dimensional diagram of the relationship between the top angle of the slip teeth and the inclination of the slip teeth and the contact pressure.

The above mechanical analysis shows the formula for solving the contact pressure between the casing and the cava during the seating and sealing conditions. As can be seen from Equation (10) and Figure 4, the top angle of the cavity tooth and the cavity tooth inclination angle have a greater impact on the contact pressure between the cavity and the casing wall, thus affecting the anchoring performance of the cavity, providing a theoretical basis for the later structural design focus.

3. Dissolvable plug slip anchoring performance evaluation index system establishment

As one of the key components of the DMP, the slip anchoring effect has an important influence on the performance of the DMP. Once the slip fails, it will directly affect oil and gas production and the safety of downhole operations. By analyzing the main failure forms of DMP mount slip, contact pressure criteria, slip strength criteria, and casing strength criteria are established to evaluate the anchoring performance of DMP mount slip.

3.1 Structural safety evaluation guidelines: strength guidelines

In the horizontal well segmentation fracturing process, the casing is bitten into by the seating force, and both the silp teeth and the casing are subjected to large stresses. At the same time, the teeth grooves on the base of the slip may be subjected to large stresses in the case of the use of a flanged shackle, and the strength of the base of the slip needs to be calibrated. In order to ensure that the DMP slip and casing are not damaged, the maximum equivalent force is used as an index to evaluate the safety of the DMP anchoring structure. The evaluation criterion is that the maximum equivalent force on the DMP slip teeth, slip base, and casing should not exceed the yield strength of the corresponding material, and the maximum equivalent force on them should be minimized to ensure the reliable anchoring of the DMP.

The formula is formulated as:

$$\sigma = \sqrt{\frac{1}{2}(\sigma_Z - \sigma_r)^2 + (\sigma_Z - \sigma_\theta)^2 + (\sigma_r - \sigma_\theta)^2} \quad (11)$$

σ ——Equivalent forces on the structure during seating and sealing.

σ_z ——Axial stresses on the structure during seating and sealing.

σ_r ——Radial stresses on the structure occur during seating and sealing.

σ_θ ——Circumferential stresses on the structure during seating and sealing.

3.2 Slip anchoring performance evaluation criteria: maximum contact pressure criterion rule

In the process of horizontal well fracturing, a large contact pressure needs to be maintained between the slip teeth and the casing wall to ensure that the DMP is firmly anchored. In this paper, the maximum contact pressure between the slip and the casing wall is used as one of the indicators to judge the anchoring performance of the DMP slip, and the maximum contact pressure criterion is established. The evaluation criteria are expressed as follows the higher the maximum contact pressure between the slip and the casing wall under the seating force, the more solid the anchoring.

3.3 Slip anchoring performance evaluation criteria: maximum contact pressure criterion rule

Horizontal well fracturing conditions are complex; shock and vibration may aggravate the downward movement of the DMP or even cause it to slip and leak the seal. When the contact pressure distribution between the slip and the casing is not uniform, it is difficult to ensure that the slip is firmly anchored, while the more uniform the contact pressure distribution between the slip and the casing, the more reliable the anchoring will be. In this paper, we establish the criterion of anchoring performance of slip contact uniformity and use the average contact pressure and standard deviation of contact pressure (S) between slip and casing as the index of contact uniformity between slip and casing. This is used to evaluate the slip's anchoring performance. The evaluation criterion is: the contact between the casing and the slip should be as uniform as possible; the greater the average contact pressure between the slip and the casing and the smaller the standard deviation of the contact pressure, the better the anchoring effect.

The formula is formulated as:

$$\bar{p} = \frac{1}{n}\sum_{i}^{n} p_i \,, \quad S = \sqrt{\frac{\sum_{i}^{n}(p_i - \bar{p})^2}{n-1}} \quad (12)$$

where, $\bar{p}$ — Average contact pressure between the slip and the inner wall of the casing.

S — Standard deviation of contact pressure on the contact surface.

p_i — contact pressure at the i-th value point.

4. Simulation analysis of the anchoring performance of dissolvable ball mount slip

4.1 Finite element modeling of soluble ball mount slip

In this paper, the DMP structure is simplified according to the working principle of DMP seating and anchoring components. This paper focuses on the effect of slip structure on the anchoring performance of DMP seating. Therefore, the seal ring and other structures are omitted, and the sliding body, slip, and casing structures are retained. Considering the symmetrical structure of the slip in the soluble ball holder, only a single slip needs to be subjected to finite element analysis to reduce the computational complexity. A meshing intelligent grid generator was used to divide the structured grid. In this paper, the sliding body is meshed by the sweep method, the mesh size of the slip base is set to 2 mm, and the mesh size of the slip block or slip nail is set to 1 mm. Face sizing is applied to the inner surface of the casing, and the grid size is set to 1.2 mm and the global grid size is set to 3 mm. The grid division is shown in Figure 5.

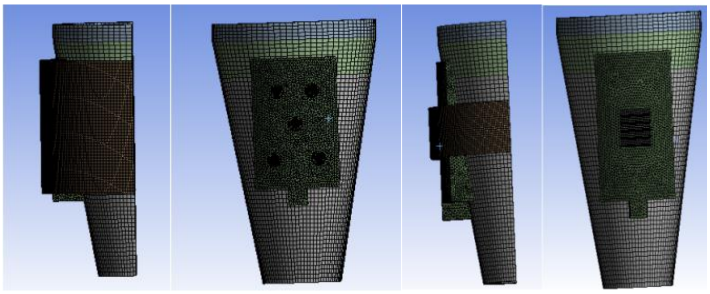

(a) Embedded slip nail (b) Embedded slip block

Fig. 5. Mesh division for simulation study of slip anchoring performance.

The material of the DMP sliding body and slip base is soluble aluminum alloy, and the material of the slip block is cemented carbide. The material parameters of each part are shown in Table 1 below.

Table 1. Material parameters of each component of the soluble ball holder.

Parts	Modulus of elasticity/MPa	Poisson's ratio	Yield strength
Slip Body	70000	0.35	350
Slip blocks/Slip nails	230000	0.26	981
Casing	210000	0.26	738

According to the working principle of DMP slip, set the side of the casing and the outer surface as a fixed constraint, and the axial displacement of the lower surface of the slip base is 0 mm. The downward displacement is applied to the upper end surface of the sliding body, and the normal displacement of the contact surface between the slip base and the base is 0 mm.
After the boundary conditions are imposed, the support reaction force at the upper surface of the sliding body is obtained for different displacements of the sliding body. The stress, strain and contact pressure between the block/nail and the casing wall are obtained when the seating force is not greater than 9t, i.e. The seating force on a slip block is not greater than 1.5t.

4.2 Analysis of calculation results

Based on the above setup, the computational analysis of the DMP slip seating process is carried out. In order to compare the performance of slips with nail type and block type, the finite element analysis was performed to grasp the stress of slip and casing wall, as well as the contact pressure between the slip and casing wall during the plug seating process.

The results show that the distribution of contact pressure between the two casing structures and the slip is shown in Fig. 6 when the seating force is less than 1.5 t. The maximum contact pressure between the slip nail and the casing wall reached 2227MPa in the use of embedded slip nails. And contact pressure distribution is more uniform at the top of the slip block teeth in contact with the casing wall, with a maximum contact pressure of 1053MPa.

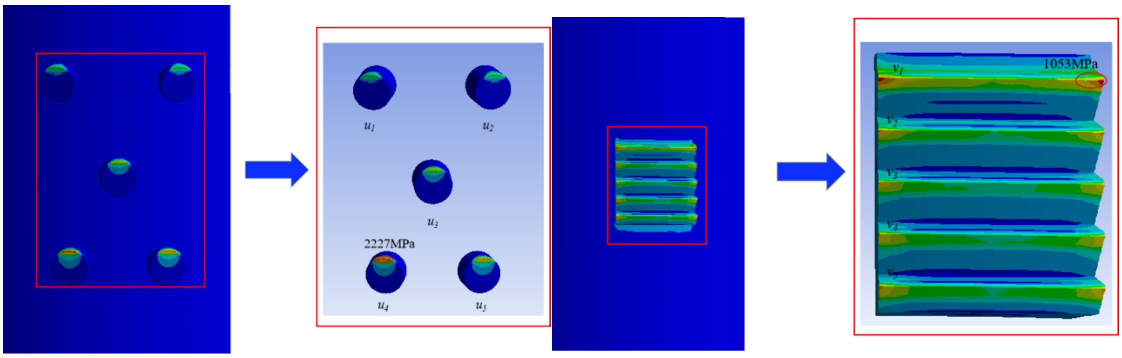

(a) embedded in the slip nail (b) embedded in the slip block

Fig. 6. Two types of structure slip and casing wall contact pressure distribution.

The contact pressure of the embedded slip nail is concentrated near the contact area, the maximum pressure of the slip nail is 1930MPa. By comparison, the contact pressure of the embedded slip block is more evenly distributed, and the maximum pressure of the slip block is 832MPa. Slip nail /slip block material yield strength are both equal to 981MPa, the maximum stress on the slip nail has far exceeded the material yield strength,slip nail may occur a large plastic deformation, resulting in slip anchoring failure.

The stress distribution of the casing wall for the two types of structural slip is shown in Fig. 7. The maximum pressure of the casing with embedded slip nails is 1212MPa, the maximum pressure of the casing with embedded slip blocks is 847MPa, and the yield strength of the casing material is 738MPa. The simulation results show that the anchoring effect of embedded slip block is better than that of embedded slip nail.

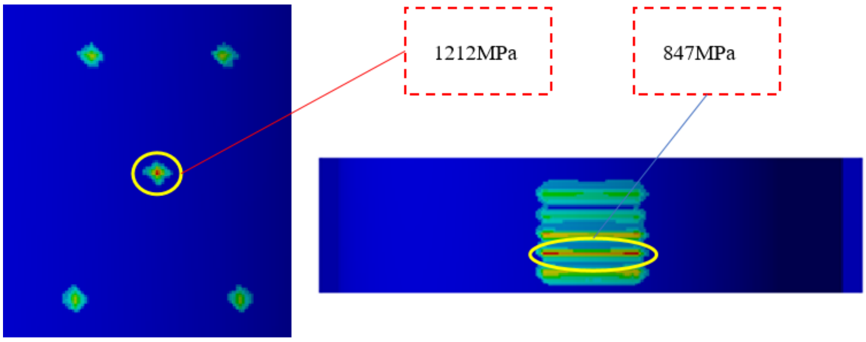

Fig. 7. Stress distribution in the wall of the two structural sleeves.

The stress distribution in the slip base is shown in Figs. 8 and 9. The maximum stress at the base of the slip is 344MPa when embedded in the slip nail and 176MPa when embedded in the slip block. The stress distribution of the five grooves is not uniform when embedded in the slip nail, and the lower part of the groove is subjected to higher stress than the upper part of the groove. The overall force in the tooth groove is even when embedded in the slip block. Slip base material has a yield strength of about 350MPa; embedded in the slip nail, slip base maximum stress is close to the yield limit; slip base may produce plastic deformation; the operation of the slip anchoring may fail.

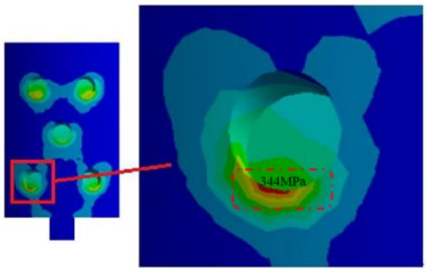

Fig. 8. Stress distribution in the base of the embedded slip nail

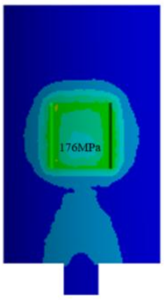

Fig. 9. Stress distribution at the base of the embedded slip block

A finite element simulation analysis of the two existing slip structures was carried out to obtain the equivalent force of the two structural slip structures. Simulation results show that when using embedded slip nail, both the slip and the casing are subjected to higher stresses, and the slip cannot be securely anchored. When using embedded slip block, slip force is more uniform and can achieve a better anchoring effect. However, there are also structural parameters for the slip block whose impact on slip anchoring performance is unclear, and the optimal combination of these parameters needs to be further explored and optimized.

4.3 Analysis of Soluble Bridge Plug Anchoring Performance Test

In order to further study and compare the anchoring performance of slip nail type and slip block type,a common electro-hydraulic servo universal testing machine was used to carry out the test and analysis of soluble bridge plug slips under simulated on-site pressurised conditions,The test aimed to test the anchoring performance by testing the damage of slip nail type and slip block type as well as the casing wall damage under the equivalent anchored seating seal loading conditions. Meanwhile, the test results were used to validate the finite element simulation calculations.

a slip nail type b slip block type

Fig. 10. Bridge plug structure with different slip forms

The experimental process is as follows:
(1)Experimental content
1)Under the same anchoring setting load,comparative test and analysis the anchoring damage of slip nail type and slip block type.
2)Under the same anchoring setting load, comparative test and analysis the casing wall damage for slip nail type and slip block type.
(2)Experimental test equipment and materials
universal testing machine 1908112 (HDT106A), slip blocks, slip nails, as shown in Figure 10, data processing equipment

Fig. 11. Microcomputer high-voltage testing system and monitoring system

Figure 11 shows the WYC Microcomputer high-voltage testing system and monitoring system,which is an automatic pressure detection device capable of automatic control for high pressure (0-100MPa) and ultra-high pressure (100-600MPa).During the bridge plug anchoring process, on the one hand,Due to the bridge plug is under the action of seating load, the damage to the slip itself will affect the stability of the anchoring.on the other hand,the degree of engagement between the slip and the casing inner wall also determines the effectiveness of the bridge plug anchoring. If the seating load is too small, the slip body fails to break,leading to seating failure.If the seating load is too large,the casing wall will suffer severe damage,which not only affects the anchoring effectiveness and sealing performance, but also poses a risk of harm to the components, impacting subsequent operations.Therefore, it is necessary to select the appropriate seating load.

In this experiment,when the seating load is 22.75MPa, the slip nail type bridge plug achieves successful seating, while the minimum load for successful seating with the slip block-type is 23.6MPa. In order to ensure the setting success, the setting load is selected as 23.6MPa in this paper for comparative test.

(3)The experimental testing procedure,as shown in Figure 12
1)Commissioning equipment, tooling fixtures: ensure the equipment and fixtures are in good working condition.
2)Equipment data acquisition system preparation: setting the values of mechanical test parameters.
3)Loading: loading the setting force on the test machine, record the sliding body stroke displacement, ensure the setting load ranges from 0 to 40MPa, and the sliding body stroke displacement range from 0 to 90mm.
4)Collection and arrangement of test results: collect setting load data, record the damage conditions of the slips and casing walls, as well as the final anchoring of the bridge plug.

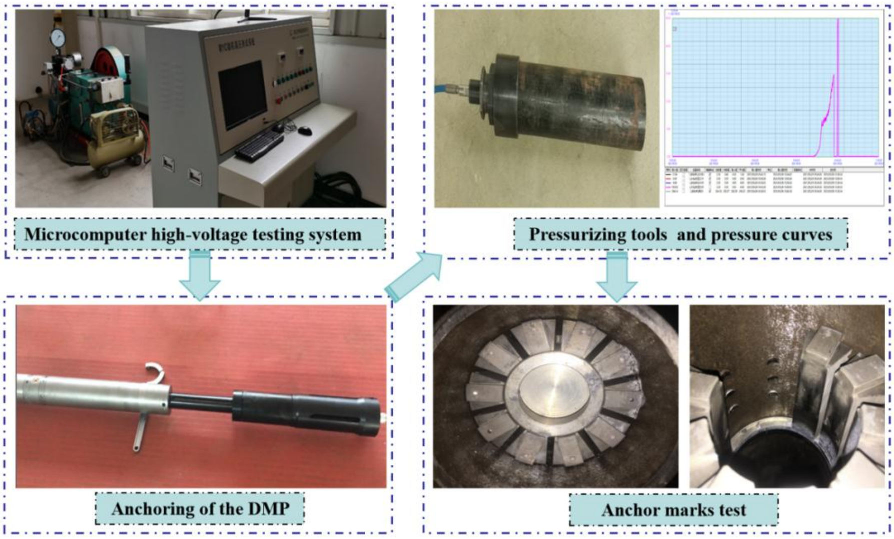

Fig. 12. Flowchart of the experimental testing procedure

(4) Analysis of the experimental results

a Embedded in the slip nail b Embedded in the slip block

Fig. 13. Two kinds of structure slip and casing wall anchoring test

The results of the comparative analysis through the slip anchoring test are as follows:

From Figure 13, the amount of damage to the inner wall of the casing can be qualitatively analyzed by using of slip nail structure in the anchoring process. The stress concentration occur in the casing wall where the slip nail biting into. Therefore, the wall of the casing will produce serious damage. Under the same force, the slip block structure produces less damage to the casing wall, which is conducive to the structural integrity of the casing wall. Besides, the damage of the slip block structure seems to be more uniform than that of the slip nail structure. The force condition of the slip block structure is better. Therefore, the comparison results proves that the slip block structure is superior to the slip nail structure.

5. Effects of DMP parameters on anchoring performance

Based on the finite element simulation results described above, the embedded slip block has better performance. The stress distribution of the slip block, casing, and slip base is relatively uniform under this structure, and the main factor affecting the anchoring capacity of the slip should be the structural parameters of the slip block. In order to further investigate the influence of the structural parameters on the anchoring ability of the slip, the parameters tooth top angle and tooth inclination angle on the slip block were selected as variables for the finite element simulation of the slip in order to investigate the optimal combination of tooth top angle and tooth inclination angle. Simulation by finite element software after changing individual parameters of the slip. By comparing the experimental results, the influence of each structural parameter of the slip on the anchoring performance can be obtained.

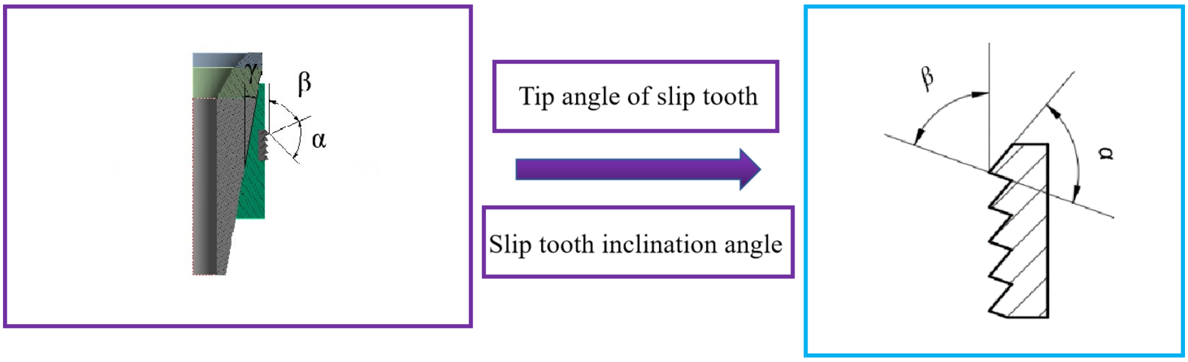

Fig.14. Slip block cross section.

5.1 Effect of slip tooth apex angle on anchoring performance

The finite element models were developed for the slip tooth apex angles of 60°, 65°, 70°, 75°, 80°, and 90°. The finite element numerical simulation is carried out to obtain the influence law of the contact pressure distribution between the slip and the casing wall under different slip tooth top angles. The contact pressure cloud diagram between the cavity and the casing wall under different slip tooth top angles is shown in Figure 15, and the contact pressure indicators between the slip and the casing are shown in Table 2.

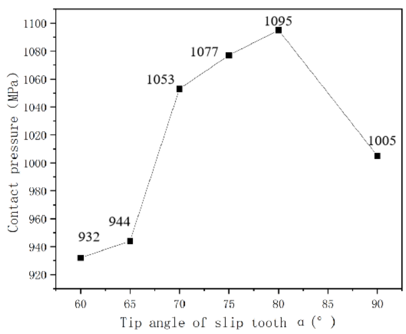

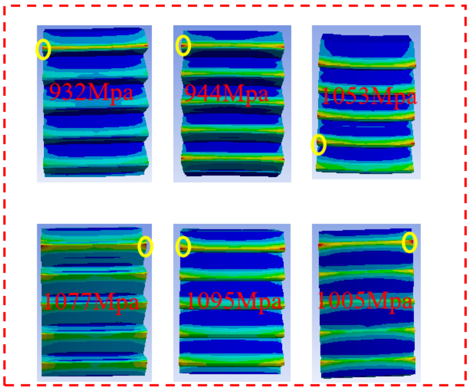

a Contact pressure curve between slip and casing b Contact nephogram of slip and casing

(1) Contact pressure diagram between slip and casing at different apex angles

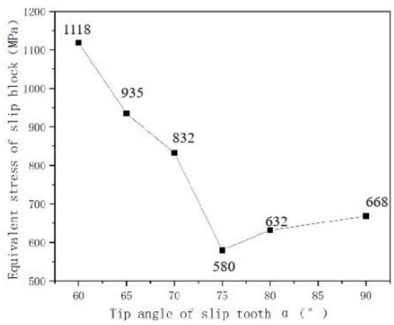

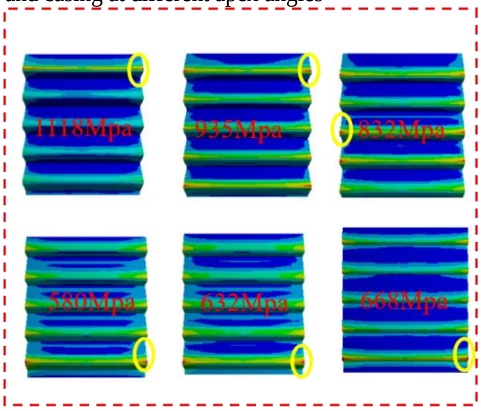

c Slip equivalent stress curve d Equivalent stress nephogram of slip

(2)Equivalent Stress Diagram of Slip under Different Apex Angles

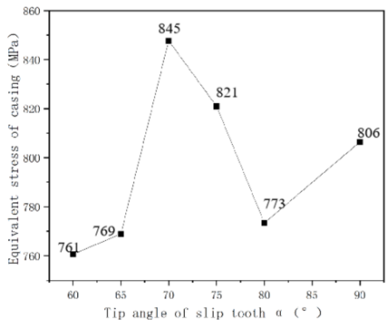

e Equivalent stress curve of casing

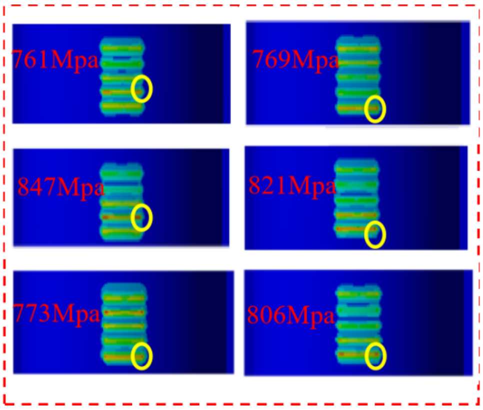

f Equivalent stress nephogram of casing

(3)Equivalent stress diagram of cannula under different apical angles

Fig.15. Stress Curve of Slip and Casing under Different Slip Tip Angles

Table 2. contact pressure indicators between the casing and the cavity at different cavity tooth top angles.

Slip tooth top cor-nerα(°)	Maximum contact pres-sure(MPa)	Average contact pres-sure(MPa)	Standard deviation of contact pres-sure
60	932	654.8	101.26
65	944	669.77	101.51
70	1053	703.54	145.14
75	1077	748.88	126.03
80	1095	773.49	125.89
90	1005	665.57	113.28

As the top angle of the slip tooth increases, the contact pressure between the slip and the casing wall tends to rise, but the maximum contact pressure between the slip and the casing decreases when the top angle of the slip tooth increases to 90°.The standard deviation of the contact pressure between the casing and the slip is the smallest when the top angle of the slip teeth is 60° and 65°, and the largest when the top angle of the slip teeth is 70°, which is still kept at a small level, and the distribution of the contact pressure between the slip and the casing is relatively uniform, without obvious stress concentration.When the angle of the top of the slip tooth is in the range of 70° to 80°, the contact pressure between the slip and the casing is higher, which is conducive to the solid anchoring of the slip.The stress distribution of the slip block at different slip tooth top angles is shown in Figure 15(2), with the increase of the slip tooth top angle, the slip block stress has a decreasing trend.At the slip top angle α=80°, the slip block stress increases compared to α=75°, but the slip block stress is still at a small level.With less stress on the slip block, the slip is safer during seating and fracturing work.In the range of 75° to 90° for the top angle of the slip teeth, the slip block is subjected to less stress and the structure is safer.The casing stress distribution is shown in Figure 15(3), and the casing stress distribution does not vary much under different slip tooth top angles.During the anchoring process of the slip, the degree of damage to the casing from the slip is small and no major damage to the casing will occur. Combined with the above analysis of the stresses on the casing, the preliminary determination of the slip tooth top angle α ranges from 75° to 90°.

5.2 Effect of slip tooth apex angle on anchoring performance

The angle of inclination of the slip teeth has a certain influence on the contact pressure of the slip on the wall of the casing. When the tilt angle of the slip teeth is too large, the slip is more difficult to bite into the casing wall, while a small tilt angle will affect the ability of the slip teeth to withstand the one-way load. Build the finite element model of the slip for the slip tooth inclination angles of 60°, 65°, 70°, 75°, and 80°. Carry out the influence of slip tooth inclination angle on cavity seating contact in order to master different slip tooth inclination angles and slip and casing wall contact pressure distribution laws.

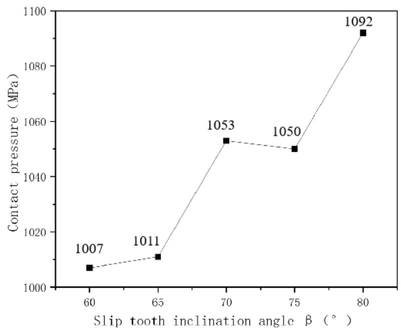

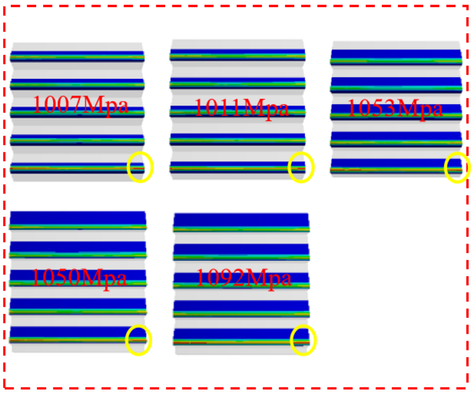

a Contact pressure curve between slip and casing b Contact nephogram of slip and casing

(1)Contact pressure diagram between slip and casing under different tooth inclination angles

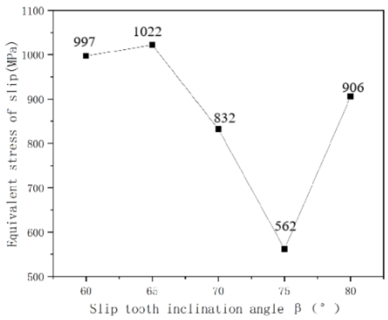

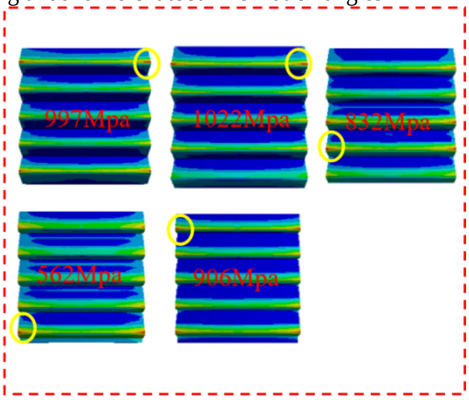

c Slip equivalent stress curve d Equivalent stress nephogram of slip

(2)Equivalent stress diagram of slip under different tooth inclination angles

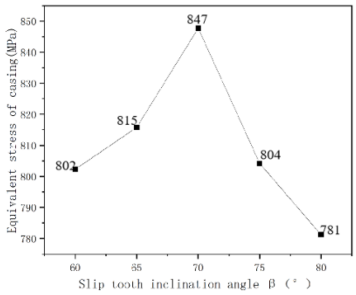

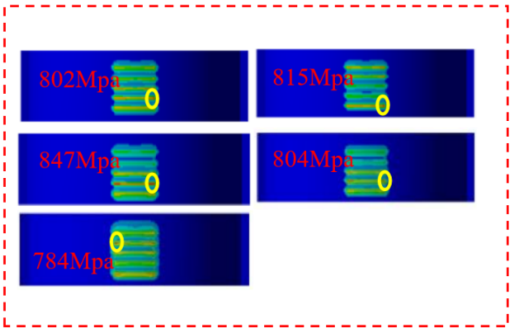

e Equivalent stress curve of casing f Equivalent stress nephogram of casing

(3)Equivalent stress diagram of cannula under different tooth inclination angles

Fig.16. Stress curve of slip and casing under different slip tooth inclination angles

Table 3. contact pressure indicators between the casing and the slip at different slip tooth inclination angles.

Slip tooth inclination β(°)	Maximum contact pressure(MPa)	Average contact pressure(MPa)	Standard deviation of contact pressure
60	1007	703.56	116.13
65	1011	716.99	104.43
70	1053	703.54	145.14
75	1050	715.74	114.29
80	1092	733.46	118.08

The contact pressure between the casing and the slip at different slip tooth inclination angles is shown in Figure 16(1), and the contact pressure indicators between the casing and the slip are shown in Table 3.With the increase of the tilt angle of the slip teeth, there is a tendency for the contact pressure between the slip and the casing to increase, but the change is small.The standard deviation of contact pressure is larger when the camber angle is 70°, and the stress of camber under different camber angles is shown in Figure

16(2).With the increase of the slip tooth inclination, the slip equivalent stress first decreases and then increases, and the slip equivalent force reaches the minimum value when the slip tooth inclination is 75°. As the slip tooth inclination angle continues to increase, the slip equivalent stress increases simultaneously.The slip tooth inclination angle of 70° and 75°, the slip structure is more secure.The casing equivalent stress at different slip tooth inclination angles are shown in Figure 16(3). The casing equivalent stress does not change much under different slip tilting angles, which can ensure that the casing is not damaged during the seating and sealing process.Combined with the analysis of the stress distribution of the shingle block at different shingle tooth inclination angles, the preferred shingle tooth inclination angle is 70° or 75° for smooth anchoring of the shingle.From the figure, it can be seen that the fifth slip tooth has a greater contact pressure with the casing than several other slip teeth, and there is a certain unevenness in the contact pressure between the slip and the casing. It is necessary to further explore the law of multi-factor influence on the force of the slip structure.

6. Structural optimization analysis of a dissolvable ball mount clutch

As mentioned above, to ensure the safety of the slip structure, the top angle of the slip teeth should be in the range of 75° to 90°, and the slip teeth inclination angle can be 70° or 75°. When the top angle of the slip tooth is 75° or 80°, the contact pressure between the slip and the casing is higher, which is conducive to the solid anchoring of the slip. In order to further study the influence of the structural parameters of the casing on the anchoring, the simulation study of the anchoring process with different combinations of parameters of the casing was carried out to grasp the distribution of the contact pressure between the casing and the casing, the distribution of the equivalent force of the casing and the distribution of the equivalent force of the casing during the anchoring process, and the combinations of structural parameters are shown in Table 4.

Table 4 Different combinations of structural parameters

Tooth top angle Tooth inclination	β=70°	β=75°
α=75°	Group 1	Group 4
α=80°	Group 2	Group 5
α=85°	Group 3	Group 6

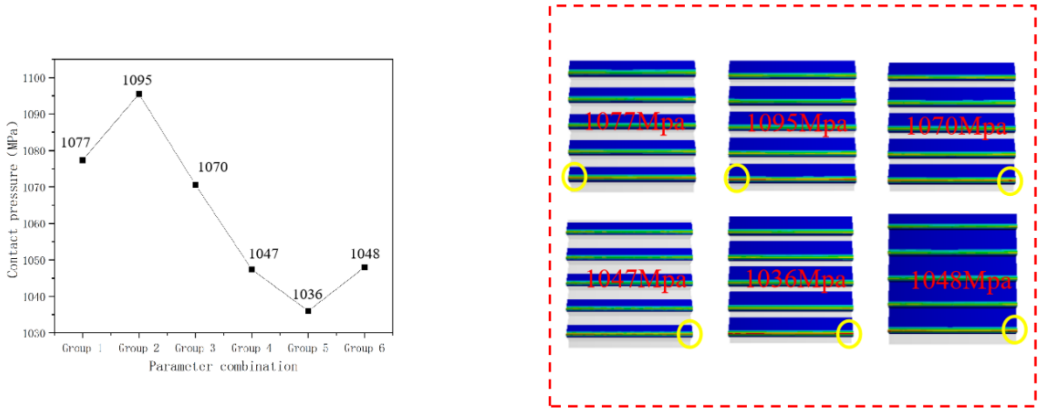

a Contact pressure curve between slip and casing b Contact nephogram of slip and casing

(1)Contact pressure diagram of slip and casing under different combinations

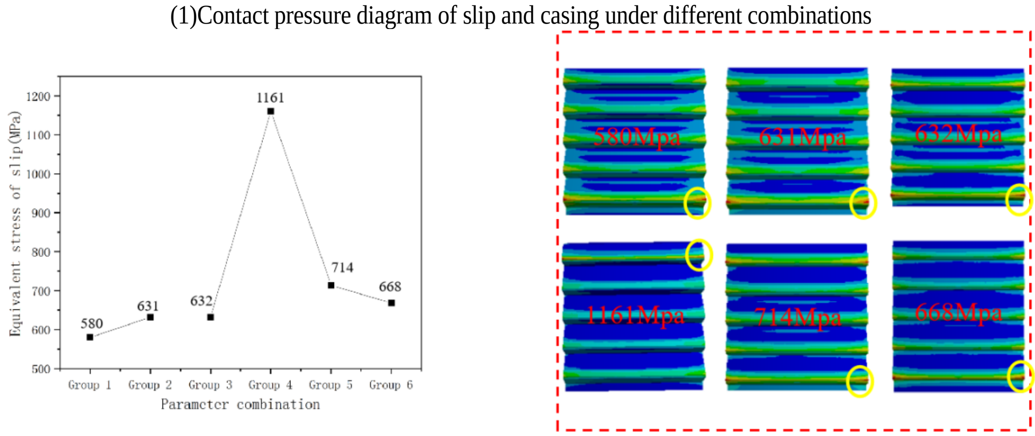

c Slip equivalent stress curve d Equivalent stress nephogram of slip

(2)Equivalent Stress Diagram of Slip under Different Combinations

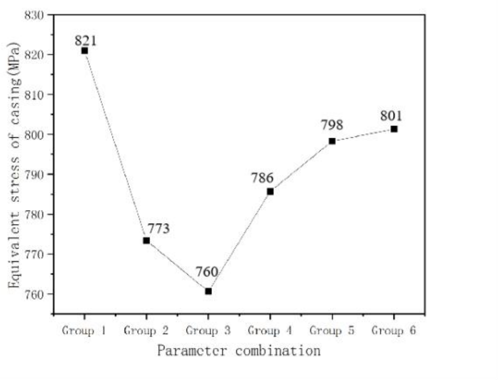

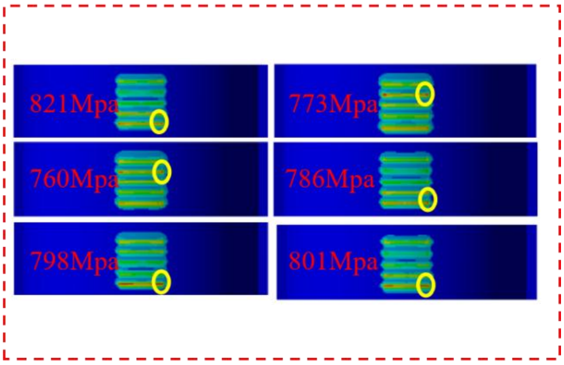

e Equivalent stress curve of casing f Equivalent stress nephogram of casing

(3)Equivalent pressure diagram of casing under different combinations

Fig.17. contact pressure between the slip and the casing wall at different slip tooth top angles.

Table 5. contact pressure indexes between the casing and the slip under different combinations of structural parameters.

Parameter combinations	Maximum contact pressure(MPa)	Average contact pressure(MPa)	Standard deviation of contact pressure
α=75°,β=70°	1077	748.88	126.03
α=80°,β=70°	1095	773.49	125.89
α=85°,β=70°	1070	797.45	107.71
α=75°,β=75°	1047	733.59	124.37
α=80°,β=75°	1036	766.62	109.75
α=85°,β=75°	1048	708.48	115.52

The distribution of the contact pressure between the casing and the slip under different combinations of slip parameters is shown in Figure 17(1), and the contact pressure indicators between the slip and the casing are shown in Table 5.The contact pressure between the slip and the casing is greater when the slip tooth inclination angle β is 75° than when the slip tooth inclination angle β is 70°.The average contact pressure is maximum for a slip tooth top angle α of 85° and a slip tooth inclination angle β of 70°.The stress distribution of the slip under different combinations of slip parameters is shown in Figure 17(2). When the slip tooth top angle α and slip tooth inclination angle β are both 75°, the slip equivalent stress is larger, and the slip may produce larger deformation to make the anchorage fail.With other combinations of parameters, the slip equivalent force is smaller and the slip structure is safer. The casing equivalent stress distribution under different combinations of slip parameters is shown in Figure 17(3). The casing stress is smaller when the slip tooth top angle α is 85° and the slip tooth inclination angle β is 70°, and the degree of damage to the casing by the slip is smaller.

Combined with the analysis of the contact pressure and stress law of casing under different combinations of casing parameters in this paper, it can be seen that when the slip tooth top angle α is 85° and tooth inclination angle β is 70°, the contact pressure between slip and casing is larger, the casing anchoring effect is good, and the stress between slip and casing is smaller, which can ensure the safety of slip in the working process, so the slip tooth top angle α is 85° and the tooth inclination angle β is 70° are preferred as the final structure parameters of the shackle.

7. Conclusions

In this paper, the anchoring performance analysis is carried out for the soluble ball mount slip structure, the finite element simulation study of the anchoring performance of the soluble ball mount slip is carried out, and the following main conclusions are obtained:

This paper analyzes the structure and working principle of DMP and the process of horizontal well segmentation fracturing with DMP. The index system for evaluating the anchoring performance of DMP was established, and the equivalent force between the slip and the casing, the maximum contact pressure between the slip and the casing, the average contact pressure, and the standard deviation of the contact pressure were used as the indexes for evaluating the anchoring performance of the slip, which provided a reference basis for the subsequent evaluation and analysis of the performance of DMP.

The finite element simulation analysis of two existing slip structures was carried out to obtain the casing contact pressure and the equivalent force on the slip and the casing for both structures. The simulation results show that the maximum contact pressure between the slip nail and the casing wall reaches 2227MPa at a seating force not greater than 1.5 t. The maximum contact pressure of the embedded slip block is 1053MPa, which shows that the slip is more evenly stressed when using the embedded slip block and can achieve a better anchoring effect.

By analyzing the structural parameters of the slip block, the influence of the slip tooth top angle and the slip tooth inclination angle on the stress state of the slip anchoring process is obtained. By comparing the force states of the casing and the slip under different combinations of parameters, the preferred angle of the top of the slip tooth is 85°, and the inclination angle of the slip tooth is 70°. With this combination of parameters, the slip is more firmly anchored, while the stress on the slip and the casing is less, ensuring that no damage occurs to the slip and casing.

Nomenclature

Q:Radial load on the interaction between the single-flap shackle and the inner wall of the slip
F_N : Positive pressure of the sliding body on the single-flap slip
F_f :Friction between the sliding body and the single-flap shackle
F_q : Friction between single-flap shackle and slip
W_Z : DMP seating load
γ : Tilt angle of contact surface between the slip and sliding body
φ : Friction angle between slip and sliding body
n: Number of slip pieces
δ: The friction angle between the slip and the casing wall
σ : Contact pressure between the slip teeth and the inner wall of the casing
A : Contact area between the slip teeth and the inner wall of the casing
m: Number of single flap slip teeth.
A: Slip teeth bite into the casing.
θ : Single-flap slip with rounded corners.
Dt: Casing inner wall diameter.
α : Slip tooth top corner.
β : Slip tooth inclination.

Acknowledgments

This research received financial support from the Shale Gas Evaluation and Exploitation Key Laboratory of Sichuan Province (YSK2022013).

References

[1] CHEN Zuo, ZENG Yijin. Present Situations and Prospects of Multi-Stage Fracturing Technology for Deep Shale Gas Development[J]. Petroleum Drilling Techniques, 2016, 44(1): 6-11. doi: 10.11911/syztjs.201601002
[2] Sun X, Dou Y, Song H, et al. Analysis of the interaction between casing and completion packer slip in HPHT wells[C]//2015 2nd International Conference on Machinery, Materials Engineering, Chemical Engineering and Biotechnology. Atlantis Press, 2015: 338-342.
[3] Dou Y, Pan H, Tong S, et al. Study on the interaction mechanism of packer slips and thick wall casing[J]. The Open Mechanical Engineering Journal, 2014, 8(1).
[4] Liu B, Cai M, Li J, et al. Application and Analysis of Fracture Simulation of the Slip of the Permanent Packer[C]//2019 International Conference on Modeling, Simulation, Optimization and Numerical Techniques (SMONT 2019). Atlantis Press, 2019: 270-274.
[5] Zheng C, Liu Z K, Wu X L, et al. Effect of structural parameters on the setting performance of plug slips during hydraulic fracturing[J]. Petroleum Science, 2022, 19(2): 731-742.
[6] Zhu Xiaohua, Chao Shengqi, Liu Zulin, et al. Structural optimization of packer slips based on experiment and numerical simulation [J]. Journal of System Simulation, 2016, 28(11): 2729-2735
[7] Chen J Y, Dou Y H, Cao Y P, et al. Application of finite element analysis in mechanics analysis of completion packer[C]//Mechanics and Mechatronics (ICMM2015) Proceedings of the 2015 International Conference on Mechanics and Mechatronics (ICMM2015). 2016: 189-194.
[8] Tang Y, Sun P, Wang G, et al. Analysis of pressure-bearing performance and optimization of structural parameters of the slip in a compression packer[J]. Science Progress, 2020, 103(1): 0036850419881106.
[9] L.Qu. Effects of the Friction Coefficient on Sealing Performance of Packer Element, 2016[C]. Atlantis Press, 2016,01.
[10] Li D X, Zhao H L, Liu X L, et al. Design of Y422 Retrievable Fracture Bridge Plug and Analysis of Slip Characteristics[C]//Advanced Materials Research. Trans Tech Publications Ltd, 2010, 139:1064-1067.
[11] Zhang F, Wang H, Yu C, et al. Design and performance experiment of staged fracturing degradable bridge plug for horizontal well[C]//Journal of Physics: Conference Series. IOP Publishing, 2021, 2044(1): 012033.
[12] Wang W G , Hong-Mei N I . Structure optimization of retrievable bridge plug slip by the combination of BP network and genetic algorithm[J]. Journal of Machine Design, 2009.
[13] Wang Y, Gao Q J, Zheng F L. Contact analysis between packer slips and casing based on abaqus[C]//Advanced Materials Research. Trans Tech Publications Ltd, 2014, 850: 262-265.